Available online at www.sciencedirect.com

ScienceDirect

Procedia Engineering 199 (2017) 3115–3120

Procedia Engineering

www.elsevier.com/locate/procedia

X International Conference on Structural Dynamics, EURODYN 2017

# The Hardanger Bridge monitoring project: Long-term monitoring results and implications on bridge design

Aksel Fenerci*[a], Ole Øiseth[a]

[a]*Dept. of Structural Eng., Norwegian University of Science and Technology, 7034 Trondheim, Norway*

**Abstract**

In design of slender suspension bridges, which are prone to wind excitation, accurate prediction of dynamic response is essential for reliable designs. However, dynamic response calculations involve many sources of uncertainty, one of which is the modeling of the gust loading. The long-term data of wind velocities and accelerations from the Hardanger Bridge monitoring project are presented here to investigate the variability in dynamic response. The buffeting response of the bridge is then evaluated in frequency domain using a multimode approach. The self-excited forces are modeled using aerodynamic derivatives obtained from free vibration tests. The modal properties of the bridge are extracted from a finite element model. The spectral densities and coherences required to describe the gust loading are modeled using design provisions. The analytical results are compared with the full-scale measurement results and the implications on design of long-span suspension bridges are discussed.


Peer-review under responsibility of the organizing committee of EURODYN 2017.

*Keywords:* long-span suspension bridge; full-scale measurement; terrain effects; buffeting analysis; frequency domain

* Corresponding author. Tel.: +4773594541.
*E-mail address:* aksel.fenerci@ntnu.no

1877-7058 
Peer-review under responsibility of the organizing committee of EURODYN 2017.
10.1016/j.proeng.2017.09.576

## 1. Introduction

The Norwegian Public Roads Administration (NPRA) is currently investigating possibilities to free its western coastal highway E39 from ferries. Straits up to almost 5 km in the Norwegian fjords have to be crossed, which calls for novel bridge designs. Suspension bridges are among the most preferred solutions when crossing such spans. Reliable design and assessment of long-span suspension bridges relies on accurate prediction of wind-induced dynamic response and this requires a solid description of the stochastic wind field at the site. In modern design codes, including the bridge design code of Norway (N400), mean wind speed is considered as the only design parameter, where other wind characteristics at the bridge site are considered deterministically using field measurements, often supported by wind tunnel terrain model tests or computational fluid dynamics simulations. However, in complex terrain, the wind filed might show variable characteristics, which depend highly on the upwind terrain properties. The wind characteristics in such complex topography, as well as its effects on the dynamic response of long-span bridges remain to be investigated.

Buffeting response prediction methods for long-span suspension bridges has been extensively studied in the past [1–4]. Despite the amount of analytical effort, very few studies exist where analytical predictions were compared to full-scale measurements [5–7]. The uncertainty involved in dynamic response prediction should be well established to design longer and more flexible suspension bridges. Especially in the cases where the surrounding topography is complex, comparisons of full-scale and analytical results are indispensable. In the current study, long-term full-scale data of acceleration response of the Hardanger Bridge is compared with analytical predictions using the methodology commonly applied in design.

## 2. Hardanger Bridge monitoring project

Hardanger Bridge is the longest suspension bridge in Norway with its main span of 1308 meters. It is located at the western coast of Norway and therefore subjected to strong natural wind. Moreover, the complex topography surrounding the bridge creates unique wind characteristic at the site. The bridge was instrumented in 2013, with a state-of-the-art monitoring system capable of continuously measuring the wind velocities and accelerations on several locations throughout the bridge axis with high accuracy. An overview of the measurement system is given in Fig. 1. In total, the measurement system consists of 9 anemometers and 20 accelerometers. Among the sensors, four accelerometers and one anemometer are located at the tower tops, where the rest is distributed along the bridge span. The measurement system is set in a way that it is triggered only when a wind speed of 15 m/s is exceeded in any of the sensors. When the measurement system is triggered to record data, the data are initially logged by means of several logger units installed inside the bridge deck and then transferred to a main data logger using Wi-Fi communication. Time synchronization of data is achieved by utilizing GPS time. The data are finally transferred to local storage units using internet connection. In the present study, 9590 10-minute long recording will be considered to study the wind field and response characteristics of the Hardanger Bridge, which were recorded between December 2013 and September 2016.

The dynamic properties of the bridge were obtained through modal analysis using a finite element model of the bridge, which was created by NPRA and used in the design of the bridge. The eigenvalue analysis were conducted under dead loads. Some of the important natural frequencies and mode shapes of the structure are listed in Table 1.

Table 1. Modal properties of the Hardanger Bridge

| Lateral | | | Vertical | | | Torsional | | |
|---|---|---|---|---|---|---|---|---|
| mode no | freq. (Hz) | description | mode no | freq. (Hz) | description | mode no | freq. (Hz) | description |
| 1 | 0.05 | 1st symm. | 3 | 0.11 | 1st asymm. | 15 | 0.36 | 1st symm. |
| 2 | 0.098 | 1st asymm. | 4 | 0.14 | 1st symm. | 26 | 0.52 | 1st asymm. |
| 5 | 0.169 | 2nd symm. | 6 | 0.197 | 2nd symm. | | | |
| | | | 7 | 0.21 | 2nd asymm. | | | |

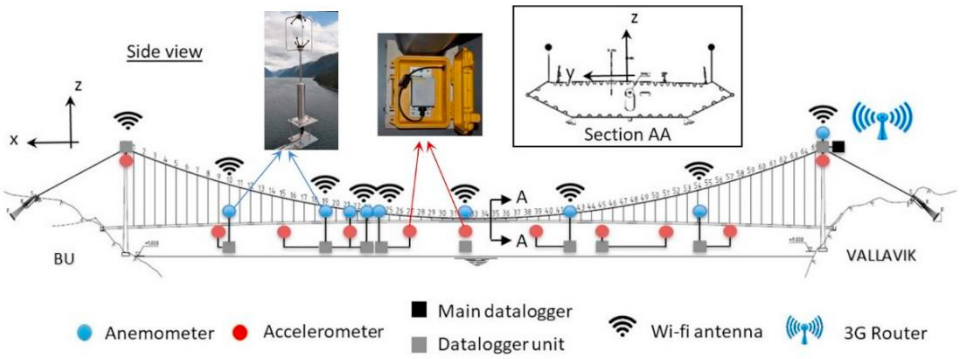


Fig. 1. Measurement system

## 3. Wind conditions at the bridge site

The wind velocities at several eight locations along the Hardanger Bridge span are sampled with 32 Hz in polar coordinates. The data were then downsampled to 20 Hz to have a common sampling frequency as the accelerometer data. A 10-minute averaging interval is selected to study the wind field statistics. The mean wind speed (U) is simply calculated by averaging the wind velocity magnitude in the horizontal plane over 10 minutes. Then, defining a coordinate system aligned in the mean wind direction, three orthogonal wind fluctuations are obtained and will be referred to as the along-wind (u), crosswind (v) and vertical (w) turbulence components. Following this notation, turbulence intensities in the along-wind ($I_u$), crosswind (Iv) and vertical (Iw) directions are calculated by dividing the standard deviation of each turbulence component by the mean wind speed.

The mean wind speed and the along-wind and vertical turbulence intensities are calculated using the wind data from the sensor approximately at the midspan (sensor A6) for all the 10-minute recordings. The results are presented in Fig. 2 and Fig. 3. in the form of wind rose scatter plots. A map showing the local topographical conditions is also provided in the background to highlight the terrain effects on the wind field. In the figures, the bridge longitudinal axis is indicated with a red straight line, which is selected as the 0° direction. Moreover, the scatter plots were color-coded to show the dependence of wind flow characteristics on the wind direction. Due to the vast number of data points, the color-coding was done using a 50x50 rectangular grid and averaging the values in each block of the grid.

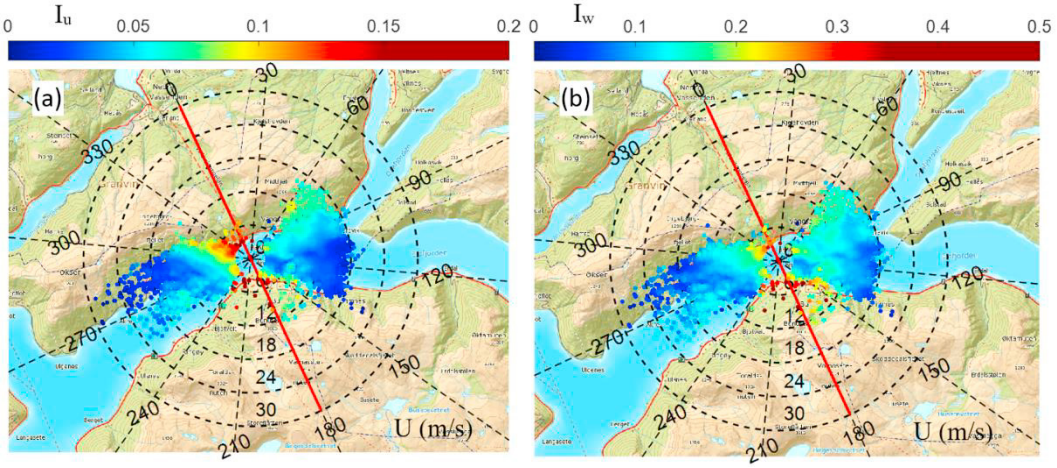


Fig. 2. Wind rose scatter plots of mean wind speed, color-coded for: (a) along-wind and (b) vertical turbulence intensity

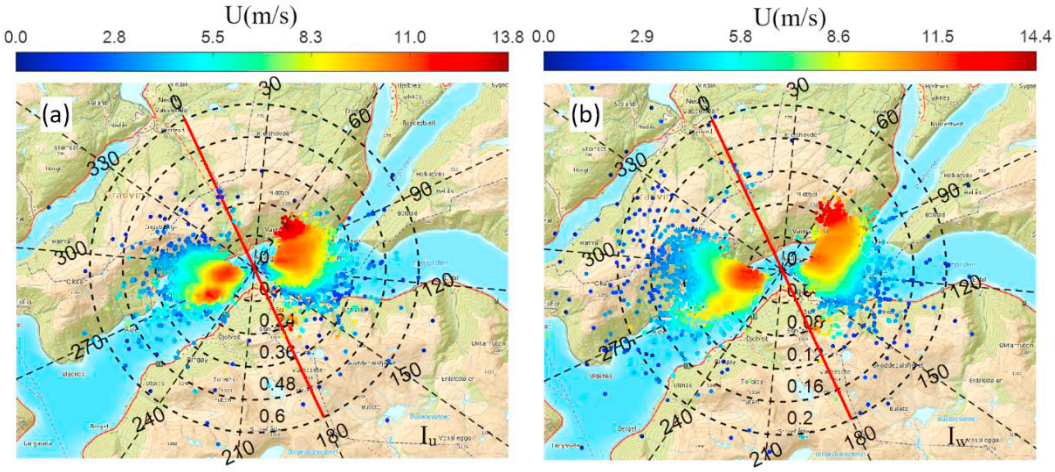


Fig. 3. Wind rose scatter plots of turbulence intensity color-coded for mean speed: (a) along-wind and (b) vertical turbulence

From the plots, it is easily observed that the surrounding terrain affects the wind field at the Hardanger Bridge site, profoundly. Fig. 2 and Fig. 3 both indicate that the along-wind and vertical turbulence intensities were higher around the mountainsides. The wind directions between 60°-90° from the east and around 300° from the west accommodate the highest turbulence intensities, due to the effect of the steep mountains in the north. The strong winds approaching from the west and along the fjord (around 270°) also indicate high levels of turbulence. The plots of turbulence intensity (Fig. 3) help better visualizing the directions where high wind speeds and turbulence intensities occur simultaneously. It is apparent that strong winds with highest levels of turbulence were approaching from the 60°-90° directional range.

## 4. Acceleration response of the bridge

The acceleration response of the Hardanger Bridge was measured using accelerometer pairs installed on each side of the girder. The data were initially sampled with 200 Hz at the site and then downsampled to 20 Hz. The lateral and vertical acceleration responses of the bridge deck were calculated by averaging the signals from the sensor pairs, while the torsional acceleration was obtained by dividing the difference of the two signals by the deck width (18.3 meters).

The root-mean-square (RMS) of the lateral ($\sigma_y$), vertical ($\sigma_z$) and the torsional ($\sigma_\theta$) acceleration components were calculated for the same 10-minute intervals, for which the wind turbulence statistics were presented. The results for the sensor pair at the midspan (H5) are plotted against the mean wind speed in Fig. 4. In the plots, the data points were color-coded for turbulence intensity, using the same method as the wind rose scatter plots. The plots indicate that the responses increase monotonically with the increasing mean wind speed, but with severe scatter. It is also seen that the high responses are often associated with high levels of turbulence intensity.

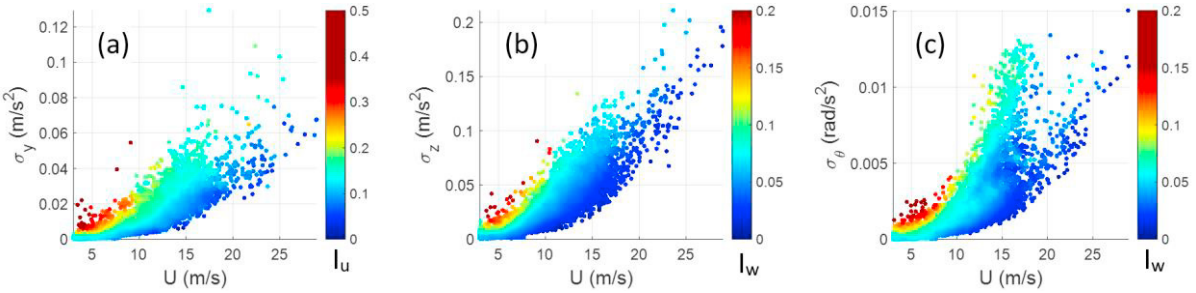


Fig. 4. RMS acceleration response vs. mean wind speed: (a) lateral, (b) vertical and (c) torsional response

## 5. Buffeting analysis in frequency domain

The buffeting response of the Hardanger Bridge was calculated in frequency domain to evaluate the performance of standard procedures commonly used in design and assessment of such long-span bridges. The multimode coupled buffeting analysis procedure previously described in [8,9] is used to calculate the response. The fully coupled system of equations, including the aeroelastic stiffness and damping terms. The mode shapes of the structure in still-air were used to define the generalized coordinates. First 100 mode shapes of the structure was included in the analysis. A modal structural damping ratio of 0.5% was assigned to all the participated modes, following the recommendation of the bridge design code of Norway (N400).

Aeroelastic stiffness and damping were modeled using aerodynamic derivatives [10], which were determined by the forced vibration tests of [11]. Aerodynamic admittance was neglected and taken as unity in the analysis.

The wind turbulence spectra were calculated using the recommendations of N400 and wind characteristics established by NPRA based on mast measurements during the design stage of the bridge. In N400, the one-point spectra of turbulence is of Kaimal [12] form, which is written as

$$\frac{fS_i}{\sigma_i^2} = \frac{a_i \hat{n}_i}{\left(1+1.5a_i\hat{n}_i\right)^{5/3}},\ \hat{n}_i = \frac{f\,{}^{x}L_i(z)}{U(z)},\ i = u,w \tag{1}$$

where f is the frequency in Hz, U is the mean wind speed, $\sigma_{u,w}$ are the standard deviations of the u and w turbulence components, ${}^{x}L_u(z)$ and ${}^{x}L_w(z)$ are the longitudinal and vertical length scales, respectively. For the Hardanger Bridge deck, of ${}^{x}L_u(z)$ and ${}^{x}L_w(z)$ are taken as 360 meters and 21 meters based on mast measurements. The spectral parameters are given as $a_u$ = 6.8 and $a_w$ = 9.4 in the design code. For the two-point turbulence statistics, the document adopts the normalized cross-spectrum formula in the exponential form [13]. The expression is written as

$$coh(f,\Delta \mathrm{x}) = \exp(-C_{u,w}\frac{f.\Delta \mathrm{x}}{U}) \tag{2}$$

where C is the decay coefficient and Δx is the span-wise separation. The decay coefficients are given as $C_u$ = 8.8 and $C_w$ = 6.3 by NPRA [14], based on field measurements. A summary of design values of wind characteristics and the mean values of the measurement data are presented in Table 2 for comparison. The design basis values of the wind characteristics show reasonable agreement with the results from the monitoring project.

Table 2. Wind field parameters

| | $a_u$ | $a_w$ | $C_u$ | $C_w$ | $I_u$ | $I_w$ |
|---|---|---|---|---|---|---|
| **Design basis** | 6.8 | 9.4 | 8.8 | 6.3 | 0.136 | 0.068 |
| **Monitoring project** | 2.6 | 6.6 | 7.6 | 7.8 | 0.165 | 0.071 |

The calculated RMS acceleration responses are compared with the measurement data in Fig. 5. The response prediction by the design method gave an underestimation of the measured lateral response, where the predictions of vertical and lateral responses were approximately in the middle of the scatter. It is seen that the design curve is exceeded by a considerable number of data points for all response components. This is because the design method does not account for the variability in the wind field. The mean wind speed is used as the only wind-related design parameter, where all the other parameters describing the wind filed are taken as deterministic values. However, in such a complex terrain, the turbulence intensities and other characteristics of the wind field show significant variability and dependence on the wind direction (Fig. 4). Compared to the other response components, the lateral response is underestimated more severely by the design curve. This might be partly explained by the absence of the buffeting force on bridge cables and towers in the analysis.

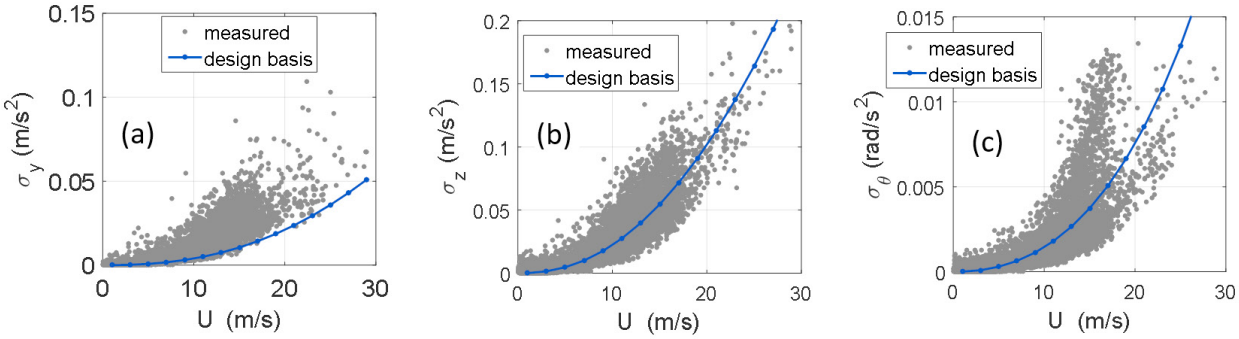


Fig. 5. RMS acceleration response compared with design prediction: (a) lateral, (b) vertical and (c) torsional response

## 6. Conclusion

Long-term monitoring data of wind velocities and accelerations from the Hardanger Bridge is used to present the wind and response characteristics. The buffeting response of the bridge is evaluated in frequency domain and compared with the full-scale measurement results. Wind field statistics showed variability and dependence on the wind direction as a result of the complex topography. The dynamic response of the bridge also showed significant variation, resembling the wind data. Analytical prediction results using the design method were generally lower than the measured response, because the design method did not capture the variable nature of the response. In complex terrain, it is essential to consider the variability in the wind field to achieve better design.

## Acknowledgements

The research described here is financially supported by the Norwegian Public Roads Administration (NPRA).

## References

[1] Davenport AG. Buffeting of a suspension bridge by storm winds. J Struct Div 1962;88:233–68.
[2] Scanlan RH. The action of flexible bridges under wind, II: Buffeting theory. J Sound Vib 1978;60. [3]Chen X, Kareem A, Matsumoto M. Multimode coupled flutter and buffeting analysis of long span bridges. J Wind Eng Ind Aerodyn 2001;89:649–64.
[4] Xu YL, Zhu LD, Xiang HF. Buffeting response of long suspension bridges to skew winds. Wind Struct An Int J 2003;6:179–96.
[5] Macdonald JHG. Evaluation of buffeting predictions of a cable-stayed bridge from full-scale measurements. J Wind Eng Ind Aerodyn 2003;91:1465–83.
[6] Xu YL, Zhu LD. Buffeting response of long-span cable-supported bridges under skew winds. Part 2: Case study. J Sound Vib 2005;281:675–97.
[7] Cheynet E, Jakobsen JB, Snæbjörnsson J. Buffeting response of a suspension bridge in complex terrain. Eng Struct 2016;128:474–87.
[8] Jain A, Jones NP, Scanlan RH. Coupled Flutter and Buffeting Analysis of Long-Span Bridges. J Struct Eng 1996;122:716–25.
[9] Øiseth O, Rönnquist A, Sigbjørnsson R. Simplified prediction of wind-induced response and stability limit of slender long-span suspension bridges, based on modified quasi-steady theory: A case study. J Wind Eng Ind Aerodyn 2010;98:730–41.
[10] Scanlan RH, Tomko JJ. Airfoil and Bridges Deck Flutter Derivatives. J Eng Mech Div 1971;97:1717–37.
[11] Siedziako B, Øiseth O, Rönnquist A. An enhanced forced vibration rig for wind tunnel testing of bridge deck section models in arbitrary motion. J Wind Eng Ind Aerodyn (in press).
[12] Kaimal JCJ, Wyngaard JCJ, Izumi Y, Coté OR, Cote OR. Spectral Characteristics of Surface-Layer Turbulence. Q J … 1972;98:563–89.
[13] Davenport AG. The spectrum of horizontal gustiness near the ground in high winds. Q J R Meteorol Soc 1961;87:194–211.
[14] Statens-Vegvesen. The Hardanger Bridge design basis - wind characteristics. 2006.